Journal of Geosciences, 71 (2026), 57–77 DOI: 10.3190/jgeosci.0056.25

Original paper

Tourmaline Crystals with Corrosion Phenomena from the Skardu Area, North Pakistan Part 1: Diversity of the outer Morphology

Paul RUSTEMEYER

Waldackerweg 7, 79194 Gundelfingen, Germany; Rustemeyer-gundelfingen@t-online.de

Innumerable dark tourmaline crystals from pockets in pegmatites around Skardu in Northern Pakistan have entered the mineral market as by-products of the trade of rare gem minerals. The author has searched this material for 40 years and thus found a great diversity of external and internal corrosion phenomena. Numerous crystals exhibit etch pits, hillocks, typical examples of which are presented from different types of crystal faces. Very special are regular linear etch grooves forming a trigonal pattern on the Pedion face and a checkerboard pattern on the adjacent trigonal pyramid face. A second group of tourmaline crystals exhibit more extreme dissolution phenomena, from crystals with a selectively dissolved pyramidal core zone, deeply etched faces with small remnants of the original external faces to the extreme of dissolving bodies. The observations of strongly corroded crystals support the model of an initially tourmaline-undersaturated hydrous fluid that separated from the pegmatite melt. The mechanisms of the formation of various etched morphologies on the tourmaline crystals as well as form-specific corrosion rates are discussed.

This part of the morphological study is the basis for the second part, in which similar corroded crystals are found as fossil complex color zones within outwardly perfect tourmaline crystals.

Keywords: Tourmaline Crystals, Corrosion Phenomena, Etching, Pegmatite, Skardu
Received: 15 December 2025; accepted: 18 August 2026; handling editor: J. Cempírek
The online version of this article (doi: 10.3190/jgeosci.0056.25) contains supplementary electronic material.

1. Introduction

Tourmaline crystals are considered excellent recorders of the formation of pegmatites for a number of reasons: they have high mechanical and chemical stability, which means they can store the information they contain through multiple geological events (Henry et al. 2003; Slack and Trumbull 2011; Dutrow and Henry 2011; Van Hinsberg et al. 2011). More than 60 different elements have been discovered in their borosilicate lattice, enabling them to estimate the enrichment of these elements in the melt and fluid during the tourmaline growth phase (Dietrich 1985; Roda-Robles et al. 2023; Li et al. 2025). Tourmaline reacts to changes in its growth environment with changes in color and shape, which are reflected in the internal morphology of the crystals as versatile color zoning (Rossman et al. 1991, Rustemeyer 2003, 2015, 2022, 2023, van Hinsberg et al. 2006).

Depending on the growth conditions, a variety of shapes and combinations arise. The diversity of the external morphology of tourmaline crystals is further increased by a variety of etching and corrosion forms – which are the subject of this study.

At the beginning of the 20th century, there was lively research regarding the etching forms of natural and artificial crystals. Studies of the behavior of crystal spheres in laboratory etching experiments were particularly popular. Tourmaline crystals were treated in such experiments with potassium hydroxide melt (Kulaszewski 1920), hydrofluoric acid or potassium bisulfate-fluorspar fusion (Honess 1929). These aggressive etching agents led to etching pits and hillocks after a short treatment of a few minutes; with a longer exposure time, the tourmaline crystal dissolved completely. This was used as a digestion method for the analysis of tourmaline crystals (Dietrich 1985). The diversity of corrosion phenomena on natural tourmaline crystals had not yet been described at that time. Accordingly, only seven of the 403 tourmaline illustrations in Victor Goldschmidt's Atlas of Crystal Forms contain references to etching phenomena (Goldschmidt 1922). The large deposits with morphologically interesting crystals from Brazil, Pakistan, Madagascar, and Namibia were not yet being mined at that time.

This morphological study is based on a collection of several thousand tourmaline crystals and more than 30,000 tourmaline thin sections. Many of the mostly dark crystals were purchased on the mineral market, which developed rapidly from the 1960s onwards due to demand from a growing number of mineral collectors. As a result, more and more tourmaline crystals were sought, found, and traded worldwide. This also led to an increase in the number of tourmaline crystals with

Published under Creative Commons Attribution-NonCommercial 4.0 International (CC BY-NC 4.0) license

interesting shapes and corrosion patterns being offered by mineral dealers. The author initially discovered the bizarre corrosion patterns of tourmalines in the 1980s on specimens from Brazil and subsequently began to search intensively for these phenomena. When processing tourmaline crystals into sets of thin sections perpendicular to the long c-axis of the tourmaline crystals, corrosion forms were found as complex color zones within tourmaline crystals that looked completely normal on the outside. They had healed completely after the corrosion process. Numerous observations of corroded tourmaline crystals and thin sections with fossil corrosion phenomena were reported in 2003 with a focus on Brazilian tourmalines (Rustemeyer 2003).

At that time, the supply of Brazilian tourmaline crystals declined sharply. In contrast, mineral mining intensified in the pegmatite areas of Pakistan and Afghanistan. The main targets of this mining were miaroles with freely crystallized colored tourmaline, aquamarine, topaz, and spodumene crystals for the collector and the gemstone market. Along with these high-priced minerals, large quantities of black tourmaline crystals from Pakistan also entered the mineral market. Most of them had freely crystallized in miaroles – many of them exhibit interesting etching and corrosion phenomena. These will be presented and discussed in the first part of this study.

The second part (Rustemeyer 2026) deals with the discovery of etching and corrosion phenomena, as described in the first part, inside tourmaline crystals that are unremarkable on the outside because they have completely healed. Both parts are illustrated with the best examples from a collection of hundreds of such tourmaline crystals and series of thin sections with etching phenomena. This is a purely morphological study, which will be further explored in collaborative projects involving analyses in the future. For ease of reference, the illustrations are labeled with the inventory numbers of the respective objects. The author would be happy to provide samples for analytical work.

Pakistani pegmatites

Almost all of the crystals described in this paper originate from miaroles in numerous pegmatite fields around the Shigar Valley in northern Pakistan. Skardu, the capital of the province of Baltistan and center of the mineral trade from the local gemstone mines, is located in the middle of this area.

In the Shigar Valley area, granitic melt intruded into fissures in the Dassu orthogneiss, creating pegmatite veins up to three meters thick and up to 4 km long (Laurs et al. 1998; Agheem et al. 2004, 2011; Jagoutz et al. 2018). Miaroles in this pegmatite yield numerous gemstone minerals (Kazmi et al. 1985; Hammer 2003; Grasemann and Dragantis 2003) such as beryl of the varieties aquamarine and morganite, topaz, tourmaline, fluorite, and apatite, as well as large quantities of schorl.

2. Observations of macroscopic etching phenomena on the faces of tourmaline crystals from the Skardu district in Pakistan

2.1. Observation method

Subtle etching phenomena on the surface of tourmaline crystals are best detected by viewing the crystal surfaces in reflective light with the naked eye, under a binocular microscope, or under a reflected light microscope.

To take the photos of the crystal surfaces, the faces in question were illuminated in such a way that they reflected the incident light almost completely. The easiest way to do this is to adjust the crystal until its surface is fully reflective and then carefully tilt it until it is just barely reflective. This brings out fine reliefs with particularly strong contours. The sharp macro photos were taken with an open aperture using the focus stacking method with a digital camera, bellows device, and a set of magnifying lenses. For aesthetic reasons, the macro photos of crystal surfaces were taken with a yellow filter in front of the light source.

To illustrate the morphology of the etching phenomena, a combination of three photos was chosen for each crystal: a view of the entire crystal with the most interesting surface, an approximately 8–10 millimeter wide section of this surface, and another approximately 2 millimeter wide, more strongly enlarged section of the surface.

From a collection of hundreds of tourmaline crystals from miaroles in Pakistani pegmatites, 40 pieces with particularly characteristic surfaces were selected for this paper. Since each type of face on tourmaline crystals develops individually different etching phenomena with matching symmetry, the crystals are classified according to their faces.

2.2. Basics of etch pits and etch hillocks

Etch pits are depressions on the crystal surface that form at relatively low undersaturation of a solvent at defects on the crystal surface. For etch pits to form, the dissolution rate perpendicular to the surface must be significantly greater than that parallel to the surface. In addition, the ablation rate of the defect-free crystal surface must be very low (Correns 1967; Kleber 1967; Heimann 1975; Sangwal 1987). In a graphical experiment (Electronic Supplementary Material ESM 1a), squares are removed along a dislocation line at removal ratios of 5 : 1, 1 : 1,

and 1 : 5; this results in a flat removal, a wide etch pit, and a narrow etch pit.

It is not uncommon to see etch pits on tourmaline surfaces, from which surface layers have been removed concentrically in flat but macroscopically visible steps from a multitude of crystal layers. This is unusual because, in contrast to crystal growth, one would expect individual atomic or molecular layers to be removed starting from the edge of the etch pit. In a periodic process, the solution repeatedly attacks the edge of the etch pit to remove a new layer package along the crystal surface. In this way, layer steps spread wave-like around the etch pits on the crystal surface (ESM 1b). This model also explains why crystals with a high density of lattice defects dissolve faster than perfectly grown crystals. An etch pit develops at each of the defects, and material dissolves layer by layer concentrically around it. The closer the etch pits are to each other as centers of surface erosion, the faster the respective layer is eroded (Heimann 1975, Lasaga and Luttge 2001, 2003). In some cases, areas of the crystal remain intact in surface areas with fewer defects, forming what are known as etch hillocks (ESM 1c).

2.3. Forms of tourmaline crystals from northern Pakistan

Figure 1 shows the most common forms (face types) of schorl crystals from northern Pakistan with a perspective view and a view perpendicular to the terminations. The most common form is the trigonal pyramid z, which is often combined with the pedion c. These crystals feature the etching grooves discussed below, which extend across both face types. They are a special etching form that occurs more frequently in the region around Skardu. The most common prism faces are the hexagonal prism c and the trigonal prism n.

The trigonal pyramids r and z have the same surface inclination; r is rotated by 60 degrees relative to z. A helpful way to distinguish between them is to refer to the prism face n, z shares a common edge with n, while r is oriented toward the pointed edge of the hexagonal prism. The trigonal pyramid r is often combined with the flatter trigonal pyramid e or the steeper o.

The occurrence of large tourmaline crystals with the ditrigonal pyramid at Leila Peak is unique worldwide. Trigonal pyramids are open forms that are positively oriented at the antilogous pole and negatively oriented at the analogous pole. They are equally oriented in relation to the crystal cross-section. Since the polarity of the tourmaline crystals could not be determined with certainty, all pyramid faces are shown as positively oriented in this paper.

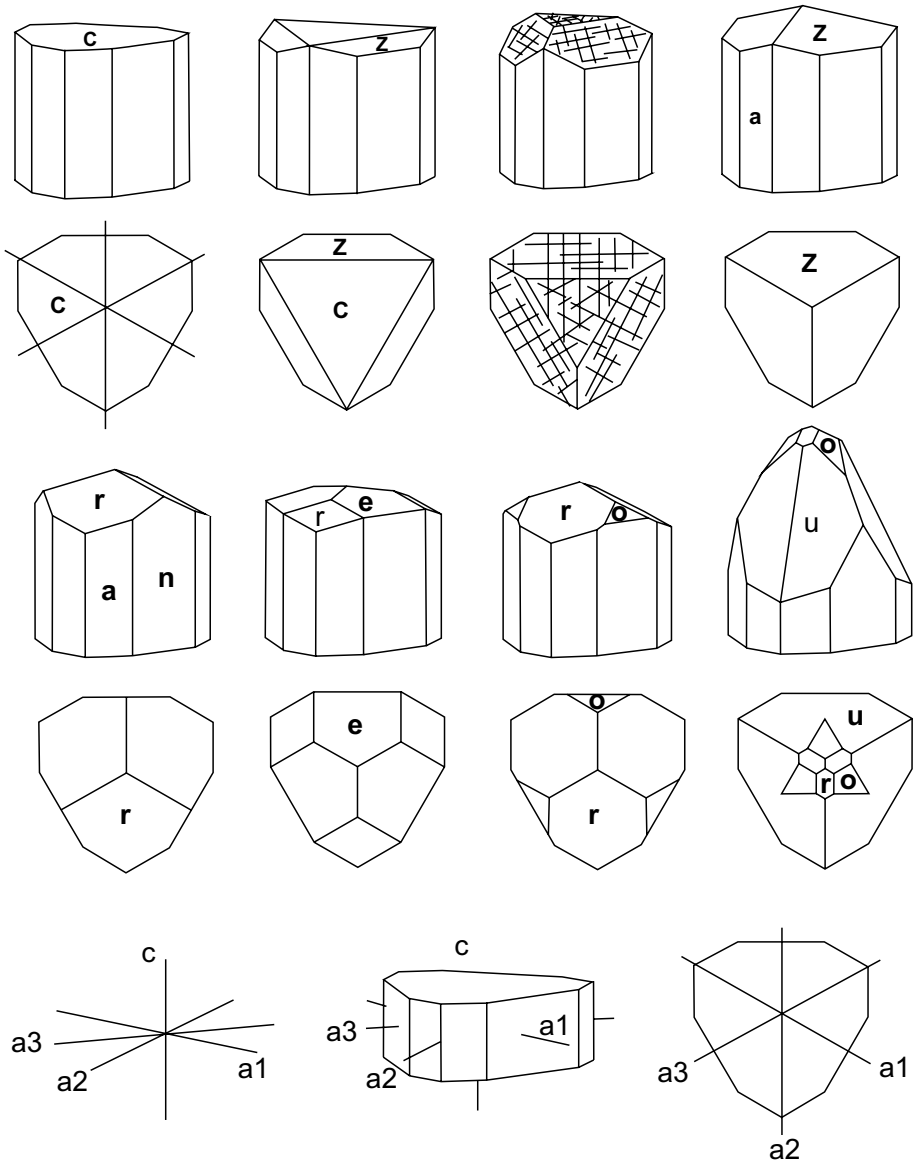


Fig. 1 a – Typical shapes of tourmaline crystals from northern Pakistan, pedion c (00.1), trigonal pyramids z (01.1), r (10.1), e (01.2), o (02.1), u (32.1), hexagonal prism a (11.0), trigonal prism n (01.0); **b –** symmetry axes of the trigonal system, c: axis of threefold symmetry, *a1-a3*: axis of twofold symmetry.

2.4. Etching phenomena on the pedion faces c

The images of etching phenomena on the pedion surface c on the Figs 2 and 3 and in the electronic supplementary material ESM 2-4 show that most tourmaline crystals exhibit several etching phenomena simultaneously. Thus, according to the predominant type of etching, tourmaline crystals with etch pits were grouped together in the first plate, hillocks in the second, and etching grooves in the third.

Etch pits – due to the threefold symmetry of this surface, triangular etch pits preferentially form on the pedion, which are oriented at an angle of 60 degrees to the outer crystal contour of the tourmaline crystal (strongly influenced by the trigonal prism n). The etch pits are in many cases arranged along dislocation lines, as is the case with the tourmaline crystals in Figs 2a–c. Many of the extensive etching grooves are also recognizable as being composed of numerous etch pits lined up next to each other. This is particularly clear in the crystal in Fig. 3h and ESM 3c. Local clusters of lattice defects may cause a dense field of etch pits in an otherwise intact surface (ESM 4a). They appear in the same shape on each type of face (form) of an etched tourmaline. The slope of the etch pit faces in many cases corresponds to a trigonal pyramid. In some crystals, such as the specimen in Fig. 2d, many such etch pits were dissolved from the pedion side by side. This creates a relief that can be interpreted either as a series of etch pits or as a relief of etch hillocks in the form of trigonal pyramids.

Numerous etch pits with less clearly defined wall inclinations form a kind of orange peel structure on dull looking pedion faces.

Etch hillocks – the surfaces of the pedions are in many cases shaped like flat landscapes consisting of rounded terraces of flat hills (Figs 3a–e and ESM 2). Almost circular hillocks with slightly dented trigonal, triangular contours protrude from them. Such a flat relief is probably created by extensive etching, in which the less defective and therefore less soluble areas of the crystal remain as etch hillocks. Interestingly, several etch hillocks may overlap. An impressive example of this is the summit of the large etching hill in crystal in Fig. 3d and ESM 2, where about 50 etching hills overlap in a small area.

Figure 3c and ESM 2c show a special example of an etch hillock. As often observed in old dissolution experiments on crystal balls, the solution eroded the material around the etching hill in such a way that an interlocking, staircase-like landscape of crystal corners and edges was created. The image of the etch hillocks in Fig. 3b (ESM 2b) is also special: on their tips, the contours of sectors of a trigonal pyramid can be observed. It is possible that a subtle recrystallization has begun here.

Etched grooves – numerous tourmaline crystals from Pakistan exhibit a net-like pattern of etched grooves on their pedion surface (Figs 3f–k and ESM 3). In a few specimens (Fig. 3f and ESM 3a), these grooves are strictly linear and aligned parallel to the axes a1, a2 and a3 (Fig. 1) of the crystal, which are perpendicular to the c-axis. More commonly they are rounded, interrupted net patterns that are only partially orientated parallel to the axes a1, a2 and a3 (Figs 3g–k and ESM 3b-e). The examples in Figs 3i, k (ESM 3d, e) show overlaps of etch grooves with etch pits.

2.5. Etching phenomena on the faces of the trigonal pyramids z

One of the most common termination face of Pakistani tourmalines is the trigonal pyramid **z**.

Etch pits – in accordance with the surface geometry, the etch pits are axially symmetrical, either as rhombuses or as isosceles triangles (Figs 3l–p and ESM 4). The walls of the etch pits on the trigonal pyramid z are often staircase-shaped, with concentric terraces spreading out from deeply etched centers, analogous to ESM 1b. Groups of etch pits are in many cases arranged along dislocations in the dip direction of face z. The heavily etched crystal in Figs 3o, p and ESM 4d, e shows beautifully terraced diamond-shaped etch pits on some areas of its fragmented pyramid z, whereas others display a terraced landscape.

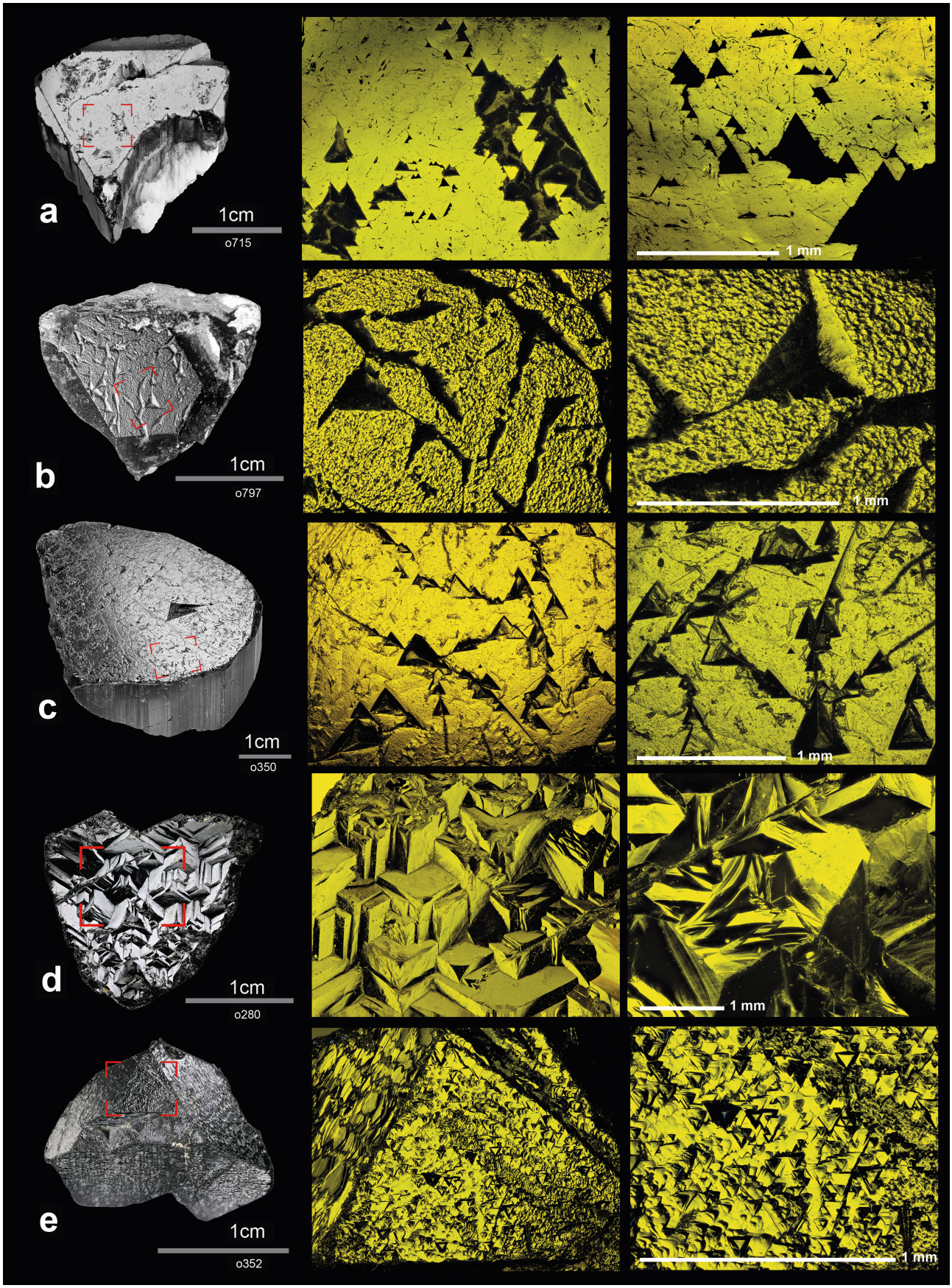
Etched grooves – as with the previously considered Pedion face, there are also different types of grooves on the faces of the pyramid z (Figs 4a–d, ESM 5a–d): some cut sharply and steeply into the crystal, others formed along a dislocation as a series of etch pits that still spread individually with diamond-shaped terraces into the area surrounding the groove.

Surprisingly, as they have not yet been seen on tourmaline crystals from other sites, there are relatively clear vertically and horizontally oriented grooves that in some cases form a checkerboard pattern (Figs 4a–c, ESM 5a–c). Such checkerboard groove patterns usually occur in crystals with a combination of trigonal pyramid faces z and the pedion c. The trigonal groove pattern discussed above (Fig. 3f) can then be found on the pedion, and the checkerboard pattern on the adjacent trigonal pyramid z (Figs 4a–c, ESM 5a–c).

Etch hillocks are rarely found on the trigonal pyramid z. One example is the rounded, scale-like elevations in

⇨

Fig. 2 Etched faces c (pedion) on schorl crystals from Skardu with etch pits on the pedion face c, left: the whole specimen. Grey bars: scale and inventory number, middle and right: macroscopic photographs of crystal faces in reflecting yellow light.


a
1cm
o715
1 mm
b
1cm
o797
1 mm
c
1cm
o350
1 mm
d
1cm
o280
1 mm
e
1cm
o352
1 mm

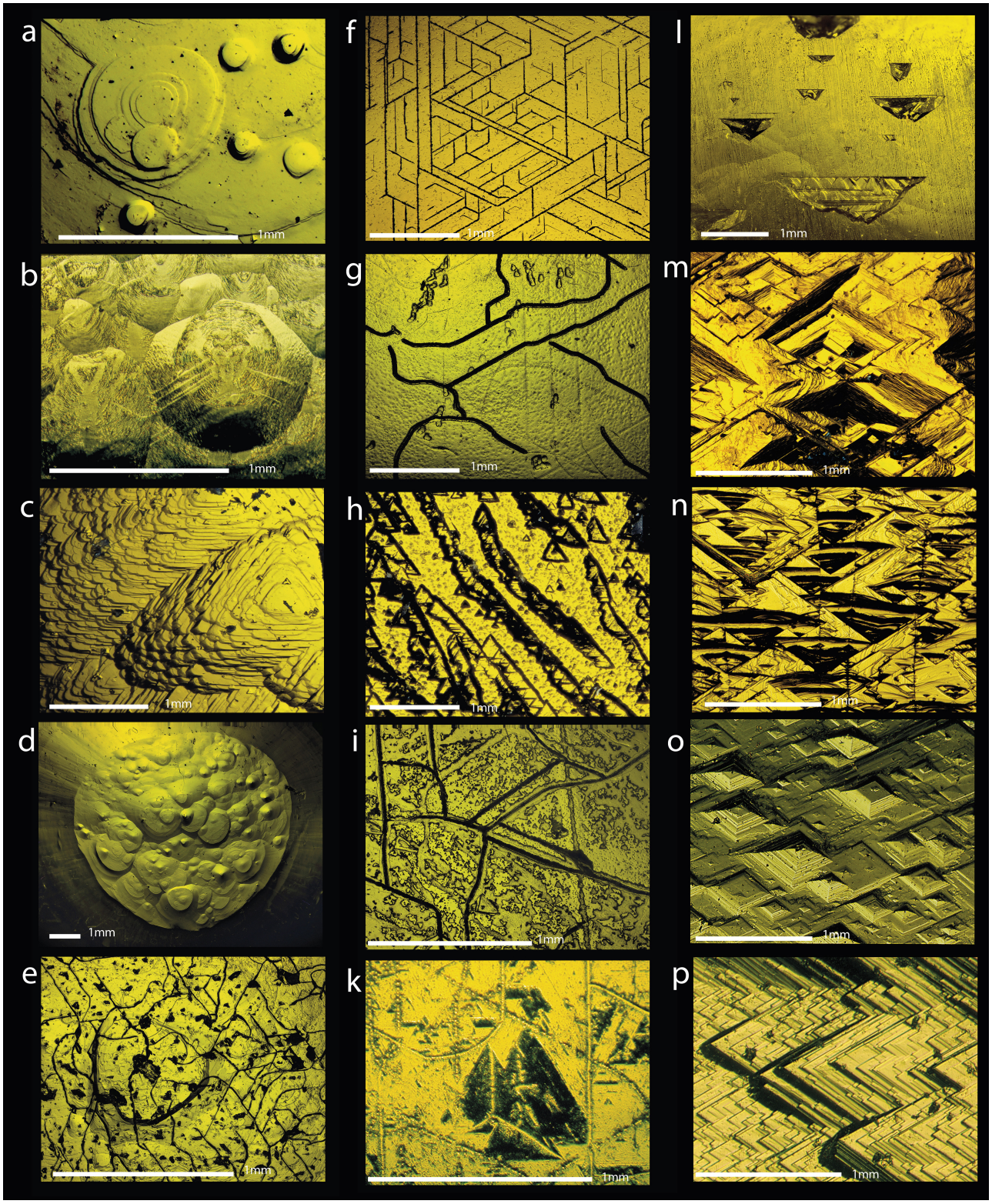


Fig. 3 Etched schorl-crystals from Skardu: **a–e** – pedion faces c with etched-out hillocks; **f–k** – pedion faces c with etched-out grooves; **l–p** – trigonal pyramid z with etched-out terraces, etch pits and an etched landscape of stairs. (Situation of the details in context of the whole specimens displayed in ESM 2, 3 and 4).

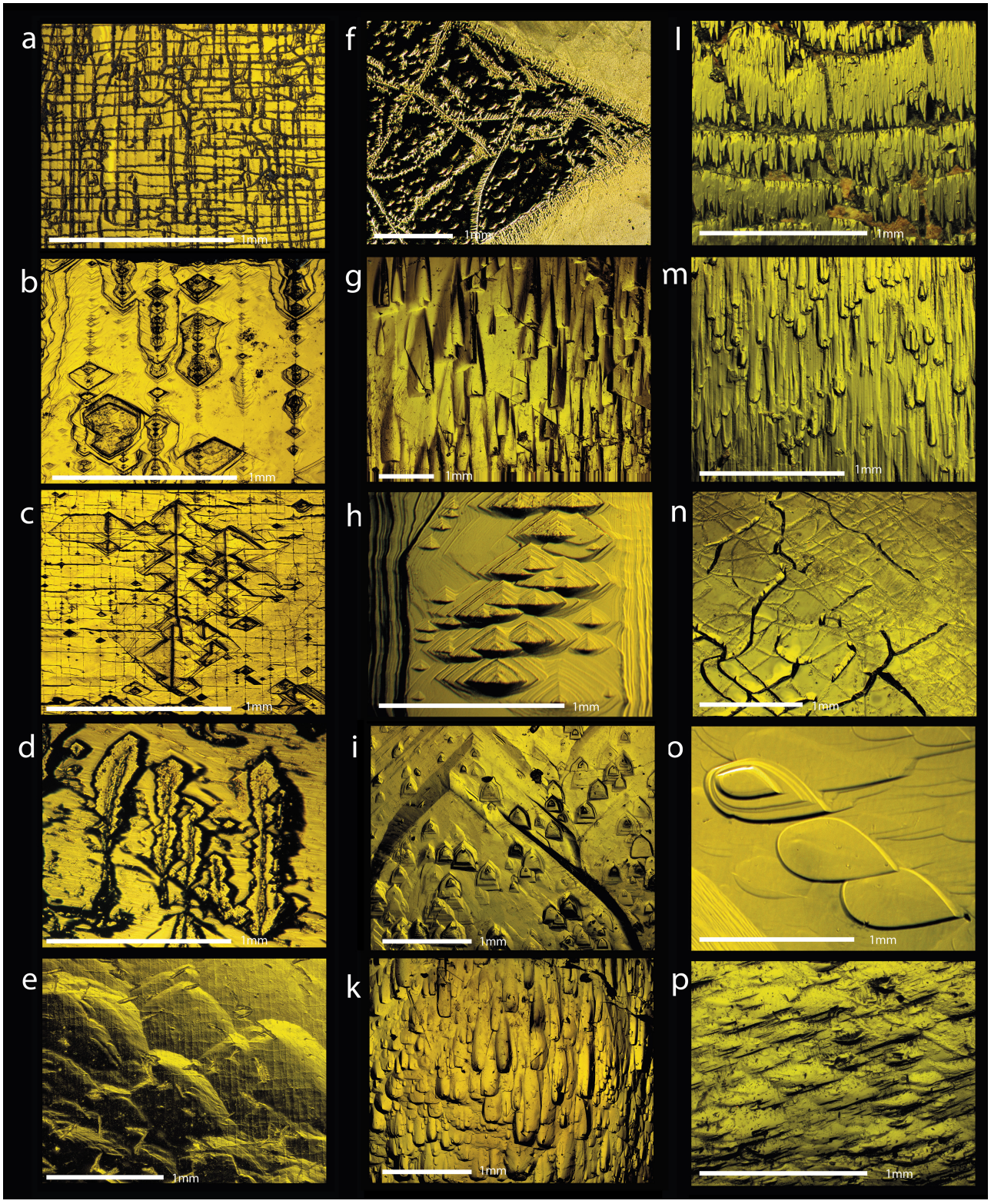


Fig. 4 Etched schorl-crystals from Skardu: **a–e** – etched trigonal pyramid z; **a–d** – with etched grooves and e with hillocks; **f** – trigonal pyramid z with etch pits; **g–k** – trigonal pyramid z with etched-out hillocks; **l–n** – trigonal pyramid e with etch pits (l), hillocks (m) and grooves (n), **o–p** – hillocks on the ditrigonal pyramid u from the Leila Peak, Pakistan. (Situation of the details in context of the whole specimens displayed in ESM 5, 6 and 7).

Fig. 4e and ESM 5e. Here, too, a superimposed checkerboard pattern can be seen in the greatly enlarged image on the right.

2.6. Etching phenomena on the surfaces of trigonal pyramids r

Etch pits are rarely found on the trigonal pyramid r. A very special example is the crystal in Fig. 4f (ESM 6a). There, numerous etch pits have formed in a triangular area of the trigonal pyramid surface. Several linear areas remained within this field of etch pits.

Typical **etch hillocks** are elongated nose-shaped elevations oriented along the fall line (Figs 4g–k, ESM 6b–e). Numerous such nose-shaped ridges can form a structure reminiscent of roof tiles. One of the most fascinating etch reliefs is the crystal in Fig. 4h (ESM 6c): deep canyons have formed along the slope line of the face. Their walls consist of layered steps. At the bottom, a series of diamond-shaped etch pits can be seen in some places. On the high plateaus between the canyons, interesting etch hillocks have formed from pyramids: their base has the shape of a distorted rhombus, which has a blunter angle at the bottom and is also made up of steps. The etch hillock formation in Fig. 4i (ESM 6d) is also interesting. In this crystal, large etch hillocks are overlain by numerous small ones; their outlines correspond to those of a Gothic church window.

2.7. Etching phenomena on the faces of trigonal pyramids g

Schörl crystals from Pakistan usually crystallize with the pyramid z. In an estimated 3% of cases, the flatter pyramid g is added, which has exactly the same slope as the edge of two pyramid faces z and is therefore rotated by 60 degrees relative to z (Fig. 1). Typical for this surface are the many narrow, nose-shaped etching ridges in Fig. 4m (and ESM 7b) with a roof tile structure. The etching grooves in Fig. 4l (and ESM 7a) are particularly noteworthy. Starting from the horizontal fault lines, elongated noses were etched out of the groove edge, more strongly upwards than downwards.

2.8. Etching phenomena on faces of the ditrigonal pyramids u

Tourmaline crystals with the steep ditrigonal pyramid u are very rare worldwide. The best location for finding them is at Leila Peak in Pakistan. Due to the low symmetry of this type of surface, the etch hillocks are shell-shaped on one side (Figs 4o, p and ESM 7d, e). Many such shells together form a roof tile structure.

2.9. Etching phenomena on the prism faces

Etching phenomena on the prism faces are very rare; these faces are obviously very resistant to corrosion. Some examples can be seen in Fig. 5. Tourmaline does not actually have any cleavability, yet irregular cracks often form, which are frequently oriented approximately perpendicular to the c-axis. From such cracks, tourmaline material is removed upwards and downwards – significantly more in the direction of the antilogous pole (*cf* 2.10). In some cases, elongated, rectangular etch pits (Fig. 5d) developed from individual defect points in the direction of the c-axis. More intensive detachment of tourmaline material results in larger caverns (Figs 5 a–c), layered etch hillocks detached from several cracks (Fig. 5e), or terraced landscapes (Fig. 5f). In more heavily corroded tourmaline crystals, the deep material removal spreads from the edges of the prism faces with the end faces towards the center of the crystal. Here, too, the removal is more pronounced from the antilogous pole.

2.10. Different etching intensity at the analogous and antilogous poles

Due to the polar crystal structure of tourmaline crystals, the terminations of the mostly elongated crystals grow in the direction of the antilogous pole about 5 to 10 times faster than the analogous pole. Accordingly, the conditions are reversed when the crystal dissolves, and the analogous pole dissolves considerably faster than the antilogous pole. ESM 8 shows one of the rare double-terminated etched schorl crystals. At the antilogous pole, the crystal of the trigonal pyramid z already has deep etch pits, while on the analogous side it has a few etch hillocks on the surfaces of the trigonal pyramid r. The steeper trigonal pyramid o on the analogous side is mirror-smooth and shows no signs of corrosion.

2.11. Investigations of the tourmaline layers beneath the surface etch groove patterns

A tourmaline crystal with a pedion face exhibiting a typical trigonally oriented groove pattern was glued onto a carrier glass with this flat face. This face was then sawn off to a thickness of approximately one millimeter and used to produce a thin section (ESM 9). ESM 9c shows a section of the original face of the crystal, and ESM 9d the corresponding section of the thin section. In it, the grooves originally present on the surface are visible as black lines. Next to this, another trigonal-oriented network of broad yellow lines can now be seen. These lines have blurred edges, which suggests a kind of bleaching, i.e., the dissolution and exchange of the dark-coloring iron against a colorless metal such as aluminum. The

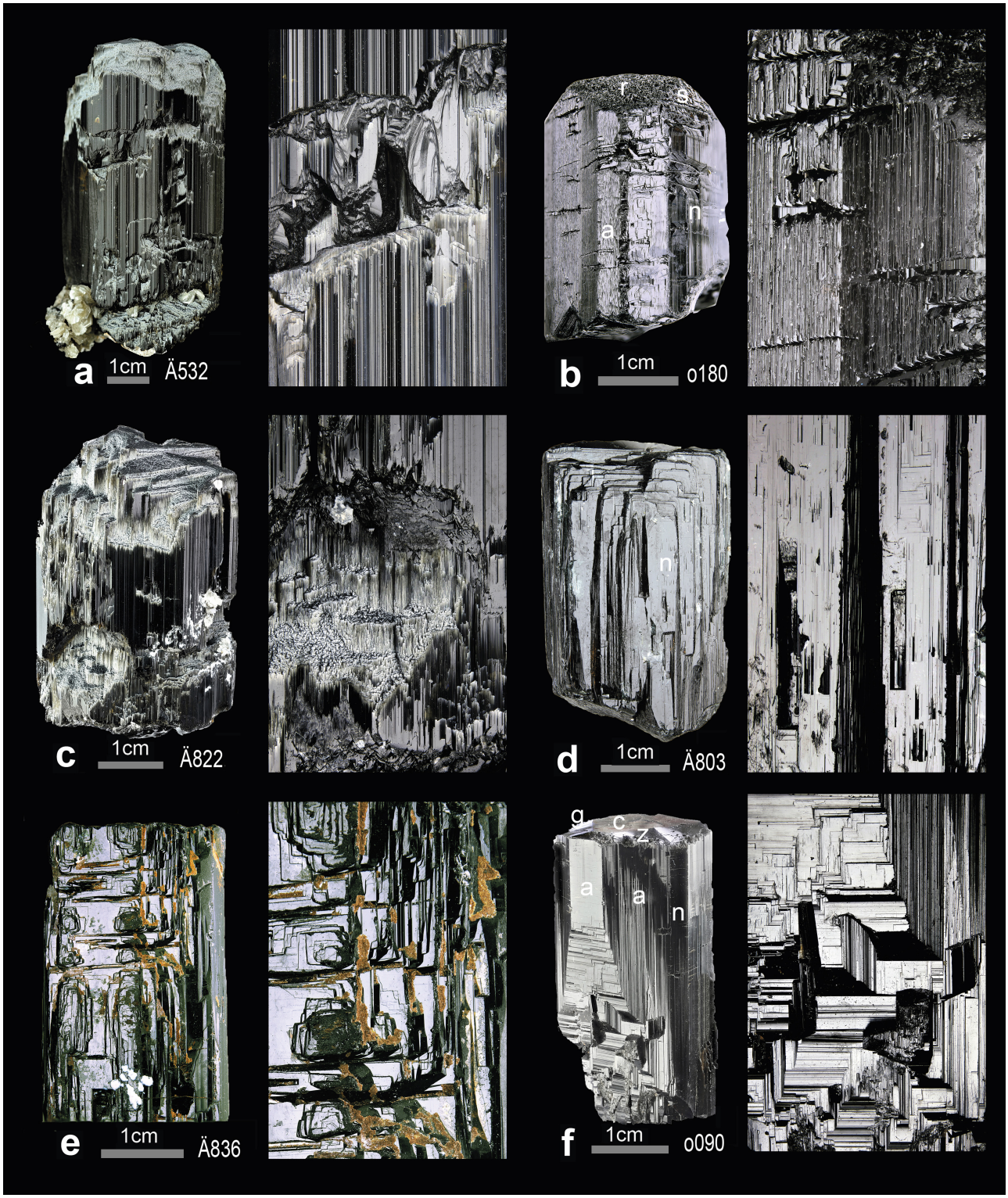


Fig. 5 Rare schorl crystals with strongly etched prism faces from Skardu: **a–f –** side view of the whole specimen and detailed image. Grey bars: scale and inventory numbers.

black lines of the groves on the surface are not surrounded by such a bleached border. The surface image shows the structure of this bright network of lines in the form of flat, barely visible depressions.

The rest of the crystal was processed into a series of slices, shown in ESM 9a, b, in order to track the phenomenon in depth. The pedion face can be seen in the bottom slice as a blue triangle. It spreads upwards

across the entire crystal cross-section in green, blue, and then green again. In the lower slices, the face of a trigonal pyramid z can be seen. It contains a typically triangular, orange-colored delta feature, i.e., a domain that has grown into this pyramid surface as a second color phase (Rustemeyer 2015, 2022). Already in the second thin section, about one millimeter from the surface, no signs of the trigonally oriented line patterns can be observed (ESM 9a, b). The entire crystal shows large, bright, irregular lines and dot structures with blurred edges on each level of the stack of thin sections. These light areas are interpreted as stress cracks, in which light dark-coloring aluminum-rich tourmaline material crystallized. For further investigation, a second crystal with larger trigonal pyramids z with a checkered groove pattern was selected. First, a thin section was prepared from the base of the crystal in order to see the entire cross-section of the crystal (Figs 6a, b). Then the tourmaline was sawn lengthwise through its center to produce a complete longitudinal section through the center of the crystal (Figs 6c, e). Finally, thin sections were prepared one after the other from the two large pyramid faces of the crystal cut at the sides (Figs 6d, f).

The combination of cross- and longitudinal-sections allows a description of the entire crystal specimen: In the cross-section, the large blue area shows the trigonal pyramid z with a small light blue triangle indicating a pedion. In addition, a delta feature can also be seen at the upper edge of this slice. The narrow edge area with the sectors of the prism faces indicates that the slice is located high up in the crystal. Figure 6c shows the top view of the longitudinal section combined with the corresponding half of the cross section. Due to the strong dichroism of ferrous tourmalines, the longitudinal section is not blue, but violet-brown in color. The light area in the middle of the longitudinal section is the sector of the pedion, which spreads upwards. Next to it, on the left and right are the dark brown areas of the trigonal pyramid z, and on the far left, several delta features are stacked on top of each other. These delta features are formed simultaneously with the growth of the trigonal pyramid z as a second color phase. These unusual color layers lie like inclined pieces of cake in the tourmaline crystal. Particularly in the area of the pedion (Fig. 6c), a horizontal layering can be seen in the longitudinal section, which corresponds to the different colors of the slices in the preceding crystal (ESM 9a, b). On closer inspection, blurred stripes running vertically through the longitudinal section, can be recognized. The black cracks in the longitudinal section were probably caused by chiseling the crystal out of the pocket.

Figures 6g and h show sections of the surfaces of the trigonal pyramids z and, below them, the corresponding sections of the thin sections made from them (Figs. 6d, f). The etched grooves visible on the face are in the same place as the bright lines in the thin section. The terraces detached from the crystal surface around the etched pits are clearly visible as brighter areas, partly because the thin section is correspondingly thinner at these points. Although the surface appears rough at the edges of the longitudinal section towards the pedion and the pyramid faces, the only structures that extend deeper are the horizontal and vertical stripes mentioned above. In both examples a superficial etching in the surface was followed by a healing with iron-poor material, which lead to this pattern of light stripes.

3. Heavily corroded tourmaline crystals

3.1. Tourmaline crystals with advanced corrosion (Fig. 16)

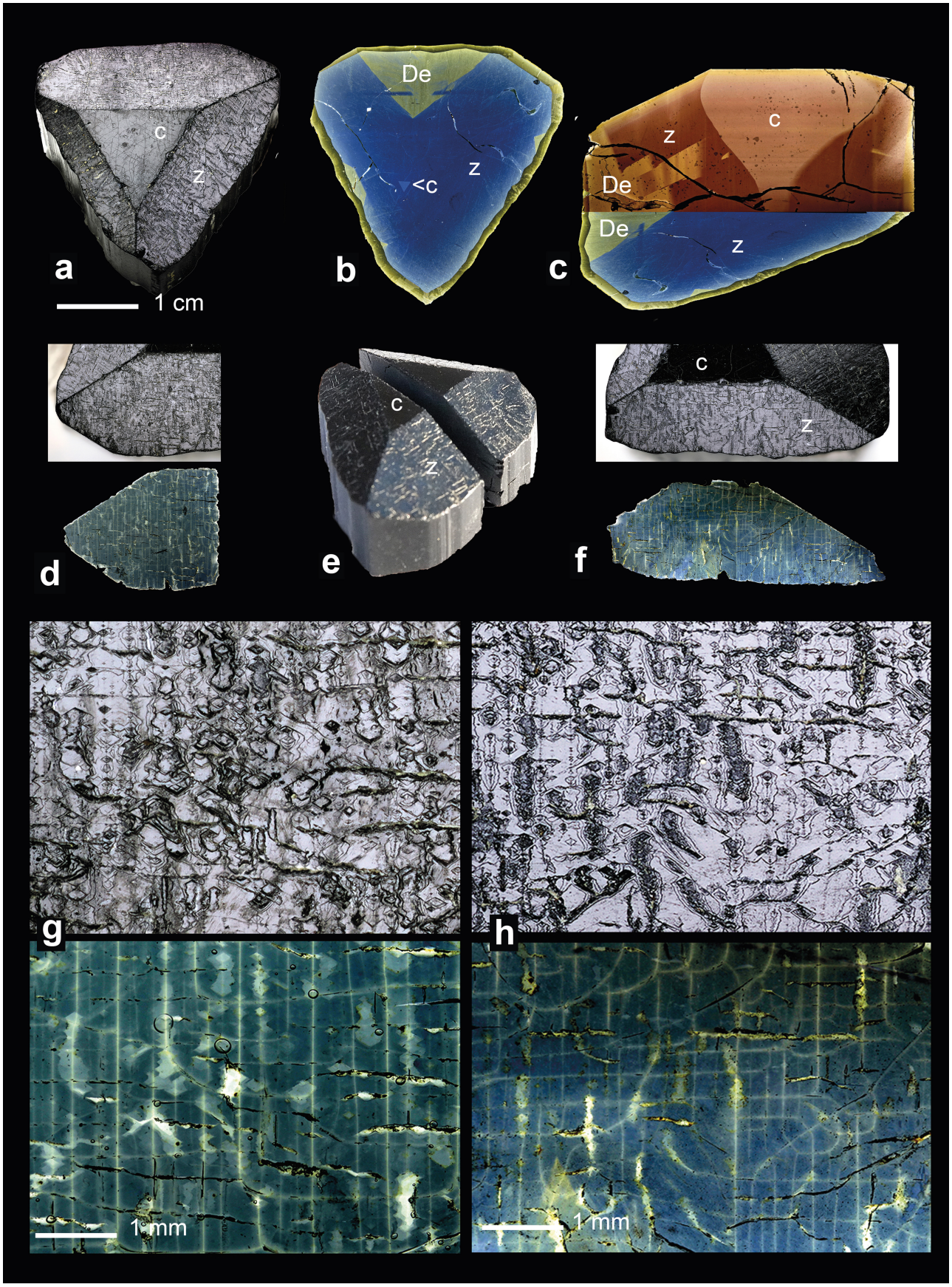
The removal of tourmaline material often goes well beyond the formation of etching pits. The terminations of the antilogous pole are particularly susceptible to attack. Since this surface grows up to ten times faster than the opposite pole in tourmaline crystals, germs with these end faces often prevail during nucleation and are therefore much more common. Corrosive dissolution is particularly severe along the edges of prism and pyramid faces (Figs 7a–c, i). The crystal retreats during corrosive attack, particularly on the pyramid face z and the prism face n. This results in a complex structure consisting of a combination of hundreds of these faces (Figs 7d–f). In addition, these faces usually exhibit a fine etching structure with etching pits, as described above. In the crystal in Fig. 7i, the small pedion c with a small part of the trigonal pyramid z is still preserved at the tip. As mentioned above, the prism faces of tourmaline crystals are significantly less susceptible to attack.

3.2. Hole etching

Some tourmaline crystals show deep holes that have been dissolved out of the core area of the crystal. Apparently, the rim area (the sectors of the prismatic faces) is considerably more resistant to intense corrosive attack than the terminations. It is always

⇨

Fig. 6 Thin sections from the etched grooves on pyramid z: **a –** the initial schorl crystal with checkered grooves on the pyramid z; **b –** a thin section of the basis of the specimen; **c –** a length cut through the center of the crystal combined with the basis cut (b); **e –** position of the length cut; **d, f –** two sections directly from the surfaces of the trigonal pyramids; **g, h –** detailed images of the crystal's surface and the same areas in the thin section.

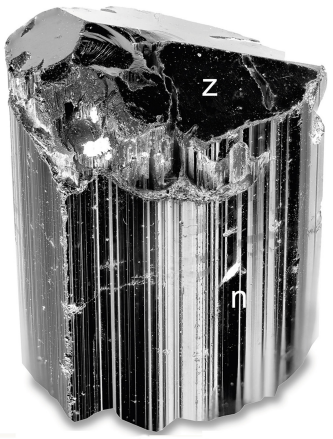

a
c
z
1 cm
b
De
z
<c
c
z
c
De
De
z
d
e
c
z
f
c
z
g
h
1 mm
1 mm



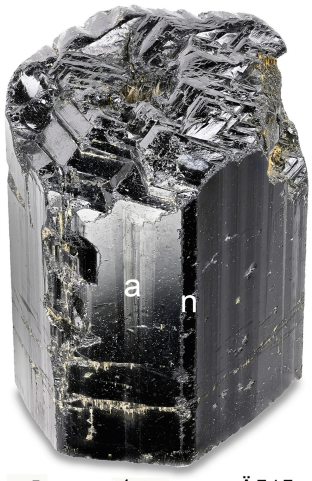
a 1cm Ä002



b 1cm Ä521



c 1cm Ä523



d 1cm Ä515



e 1cm Ä832



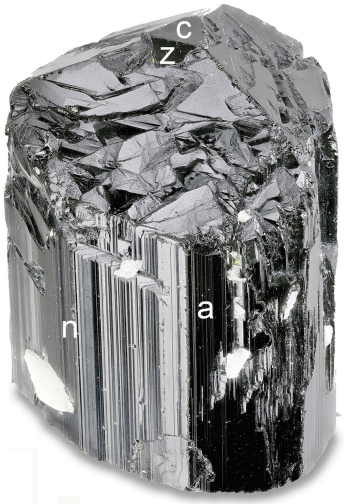
f 1cm o248



g 1cm ä525



h 1cm Ä822



i 1cm o132

astonishing to see the occurrence of thin etched-out columns and pillars that actually offer the corrosive fluid a large surface area for a dissolution process. In individual cases, almost intact parts of the terminations remained next to a deep etched hole (Figs 8g, i). In extreme cases, corrosion can create tubes up to 10 cm deep parallel to the c-axis of the crystal. Remnants of the dissolved core area from the sectors of the pyramid faces could be clearly identified in thin sections of such tubes (Rustemeyer 2015). Tourmaline crystals with hole-etching exhibit a similar fine structure in the corroded area, consisting of numerous pyramidal faces z and prism faces n.

3.3. Heavily corroded tourmaline crystals and dissolution bodies

Figure 9 shows seven examples of heavily corroded tourmaline crystals. Five of them still show clear remnants of the more resistant prismatic faces. These crystals look as if the fluid had corroded its way along the inner rim edge into the depths of the crystal, exposing the core. It is possible that large parts of the remaining rim zone on the pieces shown in Figs 9a, b, e–g broke off when the crystals were recovered. The author has found tourmaline crystals from other sites in which a narrow part of the core area has been etched away along the rim zone to form an extremely deep cleft (Rustemeyer 2015). In the crystals in Figs 9c and d, there are no remnants of the original outer surfaces; these crystals have completely retreated to their "hard cores". Such formations are also called "dissolution bodies" (Heimann 1975).

4. Discussion

The dissolution process of a crystal in a corrosive or undersaturated fluid depends on several factors, those are further discussed. These include:

– the structure of the crystal faces and their chemical composition
– the density of defects on the surface
– the composition of the fluid, its quantity and the dissolution conditions.
– the local conditions within and around the miaroles (pockets)

⇦

Fig. 7 Schorl-crystals from Skardu: **a–i –** increasing corrosion; **a–c –** with main attack in the edges of pyramidal and prism faces, and more progressive dissolution of the terminations, whilst big parts of the prism faces are still "untouched". Grey bars: scale and inventory numbers.

4.1. Factors related to the properties and structure of tourmaline crystals

4.1.1. Influence of the polar tourmaline lattice structure

The polar crystal structure probably has the greatest influence on the significant differences in the growth and dissolution rates of different tourmaline faces. The rate-limiting step in the attachment of the crystal building blocks to the tourmaline lattice is likely to be the formation of the polar six-membered silicate rings, which are all arranged horizontally in the crystal parallel to the pedion face c. As shown in Fig. 10, unlike the beryl silicate six-membered rings, the six-membered silicate rings are twisted in such a way that twelve oxygen atoms, each with a double electric charge, are located in an upper plane, and therefore only six of these oxygen atoms are located above the ring on the opposite side. This charge difference between the top and bottom causes the electric dipole properties of the silicate rings. The shape of this complex resembles a crown with six points. Since these six-membered silicate rings are all stacked parallel to each other in the tourmaline crystal, they give it its well-known polar properties such as pyroelectricity and piezoelectricity.

On the crystal surface of the upper antilogous pedion c of the tourmaline crystal, the points of the crown are positioned so that they protrude into the crystal; at the bottom on the analogous side, the oxygen atoms of the points protrude from the surface of the negative pedion – c. In the fluid surrounding the growing crystal, the silicate chains are in a dynamic equilibrium and are constantly subjected to hydrolysis and condensation reactions that continuously alter their chain structure. For entropic reasons, silicate six-membered rings are likely to occur extremely rarely and only briefly in the fluid. It therefore seems probable that the silicate rings are formed mainly through condensation on the cations of the crystal surface. To gain an idea of the geometry of the specific growth environment of a silicate ring, a silicate ring was removed from the atomic lattice model from the antilogous pedion in Fig. 10b. A group of 9 cations (six trivalent, three divalent) with a total of 24 positive charges forms a mold in which the silicate ring could condense from smaller silicate chain pieces and become electrostatically bound to its 12 negative charges. At the analogous pole (Fig. 10c), there are also 24 positive charges that can form a strong electrostatic bond with the 24 negative charges of the silicate ring. It is possible that the charge pattern of the cations on the antilogous pole is also better suited to allowing silicate chain segments to condense, thus enabling faster growth in this crystal direction. Conversely, it appears very difficult to completely remove the twelvefold charged silicate ring as a whole

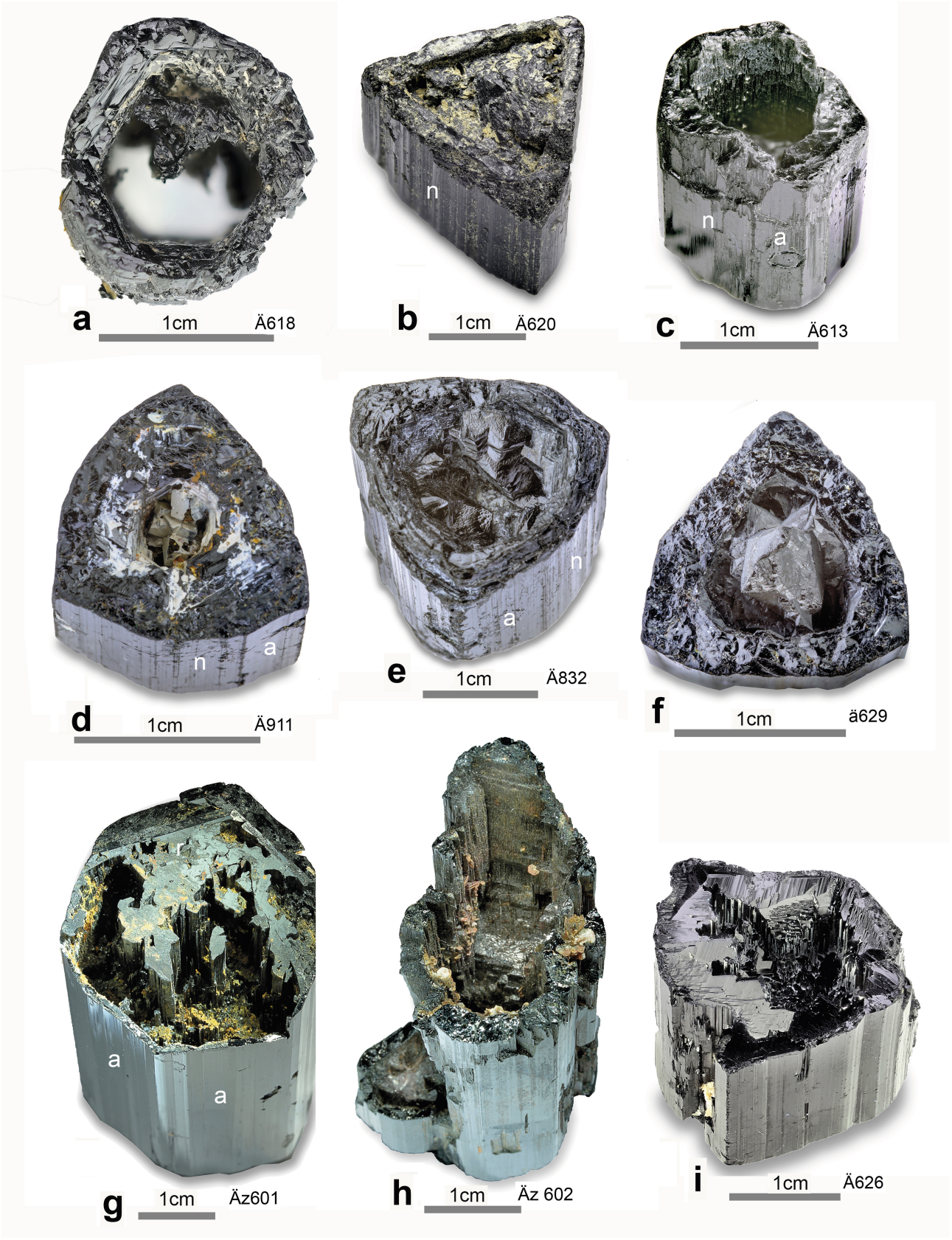


Fig. 8 Corroded schorl crystals from Skardu, Pakistan with strongly dissolved core areas; big parts of the prism faces are still “untouched”.

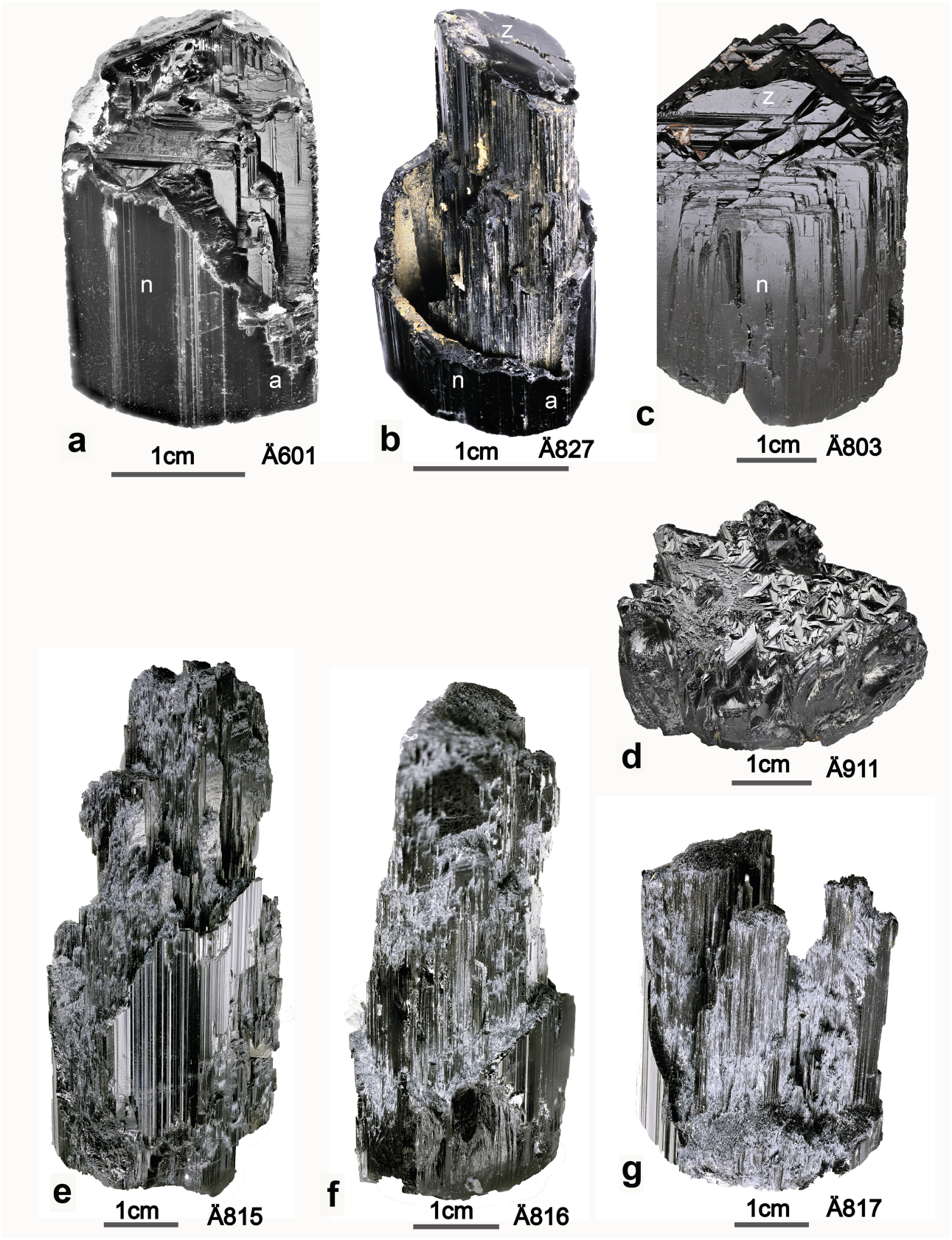


Fig. 9 Strongly corroded schorl-crystals from Skardu, Pakistan: **a, b, e, f, g –** with only small remnants of the prism faces; **c, d –** so-called dissolving bodies. Grey bars: scale and inventory numbers.

from the crystal structure when dissolving the tourmaline crystal. It is probably much easier to first hydrolyze the silicate rings and then to remove the smaller silicate pieces. Regarding the prism faces it appears extremely difficult to completely detach a silicate six-ring from the prism surface of the lattice structure, or even to come close to the silicon for hydrolysis. Accordingly, the prism faces are extremely resistant to corrosion. As discussed, in most cases they are eroded from the terminations, or from the "pseudo-terminations" that have formed in a crack in the crystal.

4.1.2. Face-specific growth and dissolution rates

According to the correspondence principle, growth and dissolution rates of crystal surfaces should correspond to each other under the same conditions (Correns 1967). Therefore, information about the crystal growth of tourmaline crystals may provide clues about the dissolution of the crystals. Longitudinal sections of tourmaline crystals, with their clearly recognizable sector zoning, illustrate the development of their growth (Rustemeyer 2003, 2015, 2022, van Hinsberg et al. 2011). At the beginning, at high temperatures, isometric crystals tend to grow, meaning that the lateral prism faces and the terminations crystallize at approximately the same rate. As the temperature cools, the growth of the prism faces slows down until it stops prematurely in the final phase. The crystal then continues to grow only at its terminations. According to the correspondence principle, this means for dissolution at lower temperatures, that the prism faces should not be attacked, or only to a minor extent.

Thin sections cut lengthwise through the center of double-ended tourmaline crystals show that the terminations of the antilogous pole often grow about

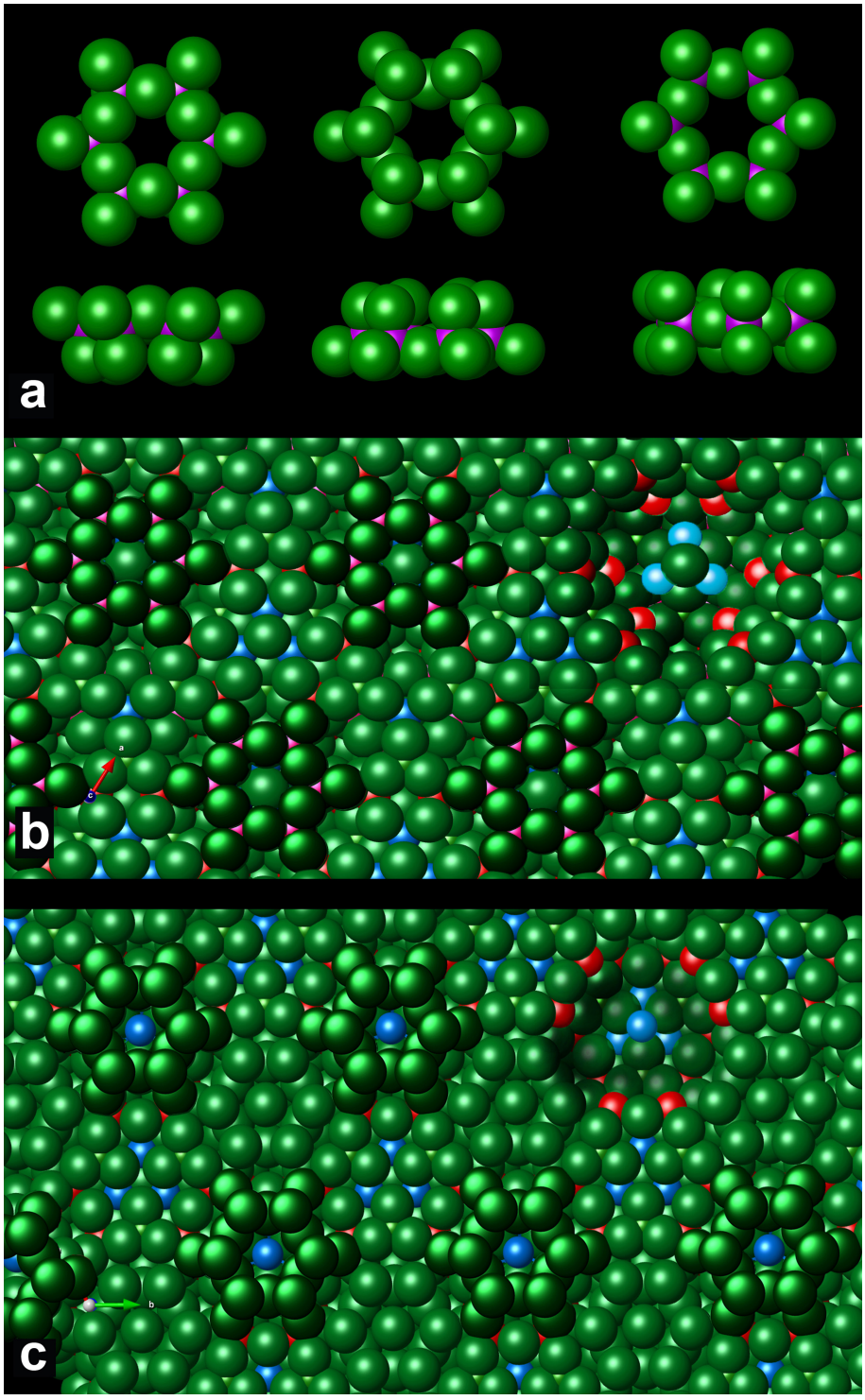


Fig. 10 a – The six-membered polar silicate ring of a tourmaline crystal (left: the antilogous pole, middle the analogous pole, right the nonpolar silicate ring from Beryll; b – antilogous surface of the positive Pedion c, the silicate rings are slightly darker, one ring is dissolved; c – analogous surface of the negative Pedion – c, the silicate rings are slightly darker, one ring is dissolved. Green - oxygen, violet - silica, red - trivalent metal (e.g. Al^{+++}), red -bivalent metal (e.g., Fe^{++}).

five to ten times faster than those of the opposite analogous pole. In the case of corrosion, the ratios are then reversed: on heavily corroded double-terminated tourmaline crystals, the antilogous pole dissolves correspondingly faster. The double-terminated crystal in ESM 8 shows this feature. Images of significantly more intensely corroded double-terminated crystals from Brazil can be found in Rustemeyer (2015). The slower growth rate of the prism faces could lead to crystal sectors with fewer defects, and this could contribute to a slower dissolution rate, too. The same argument would also explain why the faces of the analogous pole are only slightly affected.

4.1.3. Different solubility due to different composition

The numerous different kinds of tourmaline minerals have different lattice dimensions due to their different chemical compositions. This also causes differences in lattice cohesion, resulting in different melting points or solubilities (Dietrich 1985). In almost every tourmaline crystal, the sectors have a different chemical composition. This can be seen in cross-sections, both in the different chemical compositions of the sectors and often in clear color differences. In case of corrosion, these differences in solubility may lead to a selective dissolution of certain sectors from the crystal. Examples of this are colored gemstone tourmalines in which crystal cores or intermediate layers have been dissolved by natural corrosion (examples in Rustemeyer 2003, 2015). It is probable that the holes in the crystals shown in Fig. 9 formed from the same reason.

4.1.4. Internal tension in tourmaline crystals due to fluctuating composition

Tourmaline crystals can be regarded as a solid solution of various tourmaline endmembers. This compositional variability leads to the fact that numerous areas with different chemical compositions are often found within the same crystal in different sectors and growth zones. Since the chemical composition affects the different lattice dimensions and thermal expansion coefficients, this should cause internal tensions in the crystal when it is cooling down during growth. Such tension is confirmed by practical experience in the processing of transparent, crack-free tourmaline crystals. It sometimes happens that cracks suddenly form during sawing or grinding, similar to a tempered windshield that is hit by a stone. The cracks suddenly release internal tensions in the crystal.

Etching can begin on such pre-stressed surfaces or on cracks that have already formed. Such stress could also explain the formation of grooves on the etched surfaces of tourmaline crystals (Figs. 3, 4, 6 and ESM 3, 5, 9). The trigonally orientated grooves on the pedion faces and the corresponding grooves forming a checkered pattern with horizontal and vertical grooves on the adjacent pyramid faces could be attributed to tension zones running parallel to the c axis in the crystal. The longitudinal stripes observed in the longitudinal sections (Fig. 6c) could be a visible consequence of such tensions. Similarly, the horizontal etch grooves in the pyramidal faces could be attributed to stresses between thin layers superimposed on each other in the adjacent horizontal pedion faces. Indications of this layering are both horizontal striations in longitudinal sections (Fig. 6c) and the changing colors (ESM 9a, b) found in sets of thin sections below the outer pedion face.

It is not uncommon for tensions in tourmaline crystals to manifest themselves as subdivision of the crystal into mosaic blocks, which in extreme cases continue to grow as separate daughter crystals and subsequently form parallel aggregates or crystal clusters, the latter when there is a tilt angle between the blocks (Rustemeyer 2022).

There are extreme examples of narrow, several centimeters deep holes corroded parallel to the c-axis of the tourmaline crystal. They exhibit a finely structured cross section on the order of magnitude of 1 millimeter. The most extreme is the crystal shown in Fig. 8 in Rustemeyer (2026). A possible explanation is given in Heimann (1975). The formation of step and screw dislocations in a crystal can be caused by heterogeneous inclusions of different types of ions. Screw and step dislocations with Burgers vector pointing in the same direction may overlap in real crystals. In this case the dislocation can spread shaped as a narrow long spiral, forming a slim channel under tension. The reduction in tension then contributes energy to the dissolution and the formation of a deep etched-out hole. The existence of such deeply etched narrow holes and the subsequent crystallization refilling the holes without gaps (Rustemeyer 2026)) creates evidence that in this cases diffusion is not the rate-limiting step in corrosion and healing.

4.1.5. The defect density in the crystal

From an energetic point of view, an undersaturated solution is hardly able to remove building blocks from the middle of a perfectly grown crystal surface. This is why a dissolution often starts with the development of etching pits at point defects, dislocations, small-angle grain boundaries, sector boundaries, or edges of mosaic blocks (Heimann 1975). At such locations, crystal building blocks are only partially embedded in the crystal lattice, are often subject to mechanical stress, and can thus be dissolved out of the crystal structure by the solvent. Thus, the intensity and extent of the lattice defects and their density strongly determine the dissolution rate.

4.2. Influences of the fluid

Solubility of tourmaline refers to the ability of the fluid to break down silicate structures, to form soluble complexes with the ions in the tourmaline lattice, to absorb a high concentration of dissolved tourmaline building blocks, and to enable a concentration equilibrium of the dissolved substances in the miarole through rapid diffusion. The pH value of the liquid and its content of complex-forming and viscosity-reducing components such as fluoride, chloride, and borate therefore play a role.

4.2.1. Viscosity of the fluid

Based on their experimental investigation results of inclusions in quartz crystals, Thomas and Davidson (2012) report that high water concentrations can occur in pegmatite, forming melts by which the silica chains are depolymerized and remarkably low viscosities may occur especially if other viscosity-reducing and depolymerizing components ions such as fluoride, phosphate, borate, and carbon dioxide are present. (London 2008; Simmons et al. 2022). This is in line with the observation that diffusion is not the rate-limiting process, when deep holes are etched into the tourmaline crystal.

4.2.2. Extraneous substance adsorption

The presence of inhibiting foreign substances, impurities that preferentially deposit on certain crystal faces as thin layer, are able to effectively protect faces from solvent attack. Experiments have shown that such inhibitors can also have a strong influence on the shape of etch pits on the different crystal faces (Heimann 1975). Sharply defined, deeply eroded holes and fine columns of material from the original crystal, spared from corrosion, in many corroded tourmaline crystals (Fig. 8 and many examples in Rustemeyer (2026)) make the presence of surface-passivating foreign substances seem likely.

4.2.3. The absorption capacity of the fluid: undersaturation and quantity

An eminently important parameter in the etching and corrosion of crystals is the undersaturation of the fluid and the available quantity of the fluid. Together, these two factors determine how much material can be removed from the crystal. From crystal growth, it is known that increasing supersaturation leads to the formation of different areas of crystallization: normal crystal growth on the surface, skeletal growth, and dendritic growth at maximum supersaturation. In a similar way, there are certainly transitions in the dissolution of crystals that lead to different morphologies of the corroded crystals.

The driving force behind corrosion is composed of the degree of undersaturation of the fluid, the amount of available fluid, its dissolving power, and a sufficiently low viscosity that enables the necessary diffusion processes. The states with increasing dissolving power would then be:

– formation of etch pits and hillocks
– stronger dissolution of the crystal edges pyramid/prism,
– deep corrosion of larger sculptured etched faces down to the dissolution body,
– and finally strong corrosion removal with irregular etching structure without clear crystallographic faces.

4.3. Possible reasons for the corrosion of tourmalines in miaroles

Heavy corrosion and light etching are probably caused in the context of different events in the evolution of a miarole in a pegmatite vein.

4.3.1. Transition melt – supercritical aqueous fluid – hydrothermal solution

Pegmatite veins form when granitic melt at a temperature of around 700 degrees Celsius (London 2016) penetrates fissures in colder surrounding rock. As the melt cools, the granitic minerals quartz, feldspar, and mica crystallize; Borate, fluoride, beryllium, and lithium ions as well as water concentrate in the residual melt. When the concentration of borate exceeds a certain limit, tourmaline crystals begin to crystallize (London 1986, 2008, 2013, 2016 , Webber et al. 1999; Simmons et al. 2022). As cooling and crystallization progresses, the water content of the melt rises above its maximum water solubility limit. Consequently, a supercritical aqueous fluid exsolves from the melt as a second phase. This still has a high dissolving power for minerals. Thus, apparently for a time, tourmaline supersaturation coexists in the melt in the miarole and, at the same time, undersaturation in the supercritical aqueous phase (Fig. 11), which is likely to dissolve the newly grown tourmalines.

It may happen that a tourmaline crystal only partially protrudes into the bubble of supercritical aqueous fluid and is therefore only partially severely corroded – as some of the examples shown in Figs 7–9. A miarole can be regarded as a closed system, at least for some part of its history. As shown in the second part of this paper, the dissolved tourmaline substance in the miarole may recrystallize on the corroded tourmaline crystals in the aqueous phase during further cooling, completely healing them.

The separation of supercritical fluid from the melt is associated with an increase in volume. According

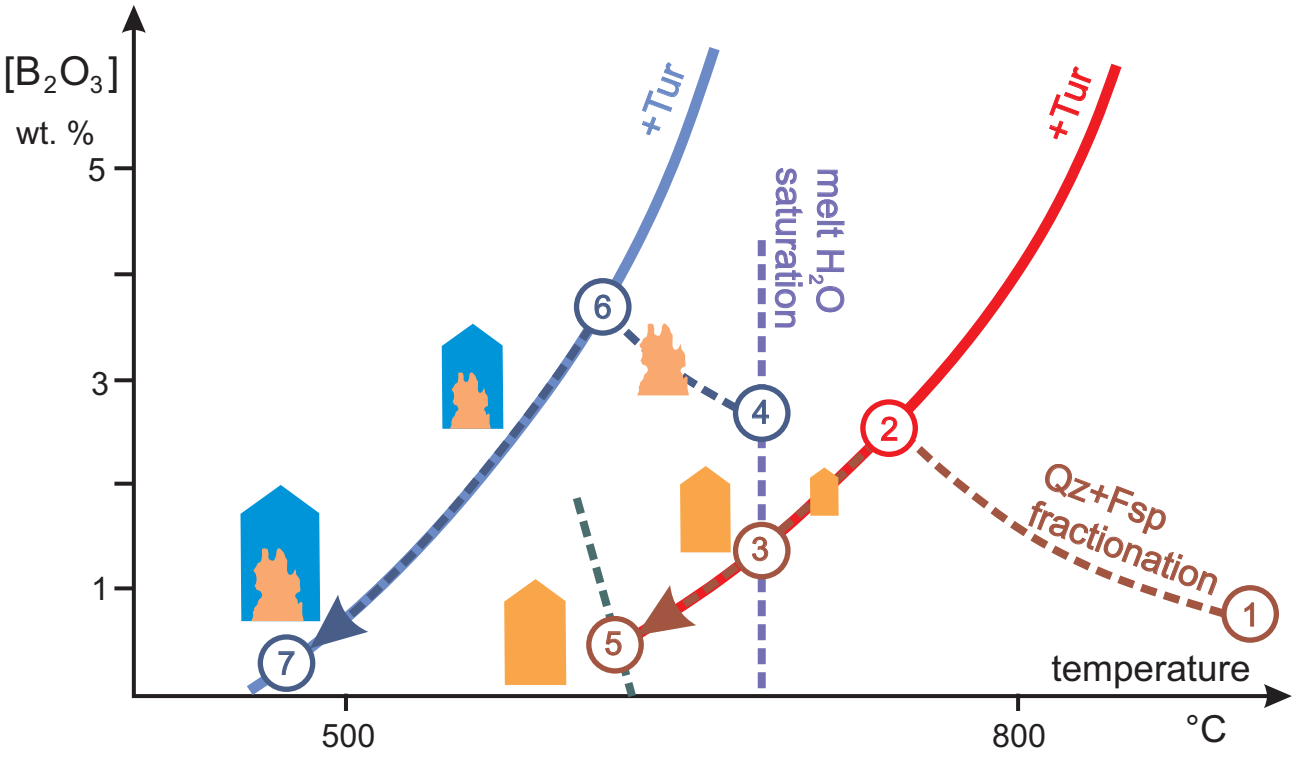


Fig. 11 Development of a crystallizing pegmatite melt:
(1) Quartz and feldspars crystallize as the magma cools. B is incompatible and [B_2O_3] of the melt increases. The melt is not saturated in Tur; no Tur is formed.
(2) Tur saturation in the melt is reached and Tur starts to crystallize from the melt
(2→3) Tur crystallizes from the melt. [B_2O_3] of the melt decreases along the Tur saturation curve.
(3) Melt reaches H_2O saturation and an aqueous fluid exsolves from the melt. [B_2O_3] of the melt stays at the Tur saturation curve, but...
(4) [B_2O_3] in the fluid is higher than in the melt according to B fluid/melt partitioning.
(4→6) The fluid is undersaturated in Tur and existing Tur gets corroded. [B_2O_3] of the fluid increases.
(3→5) At the same time, the melt is still saturated in Tur and Tur crystallization from the melt continues. [B_2O_3] of the melt decreases along the Tur saturation curve.
(5) The melt solidus is reached; the last melt crystallizes (no further Tur crystallization from melt)
(6) Tur saturation in the fluid is reached and Tur starts to crystallize/anneal from the fluid
(6→7) Tur crystallizes from the fluid. [B_2O_3] of the fluid decreases along the Tur solubility curve.
(Graphic combined from a sketch from Marschall 2026 and a publication from London 2016)

to London (2016), the pressure in the miarole may become so high that the pegmatite vein ruptures and the fluid escapes. In this way, the heavily etched tourmalines could be preserved in the miarole without subsequent healing. However, tectonic events could also cause the rock with the pegmatite vein to tear open, and a miarole creates a weakened point in the vein. Such a crack would allow the fluid to escape. And then corroded, unhealed tourmaline crystals like in Figs 7–9 are left behind in the pocket. If undisturbed, the supercritical aqueous phase remains in the miarole, where it causes transport and crystallization processes and eventually transforms into a subcritical aqueous phase at lower temperatures. With cooling, also etched tourmaline crystals will continue to grow and morph into perfect crystals with reflective surfaces. The size of the miarole is finally determined by the volume of the liquid.

4.3.2. Etch pits, hillocks and grooves as product of a late stage corrosion

The literature on formation conditions of the subtler final etch phenomena (etch pits, hillocks and grooves) on the surface of fully crystallized tourmaline crystals is rather scarce. Therefore, several possibilities can be discussed:

– Microthermometric investigations of liquid inclusions that formed simultaneously with crystallized melt inclusions showed that phases with very high alkali content may form in pegmatites (Thomas et al. 2012). Analogous to the experiments by Kulaszewski (1920), who observed etch hillocks and pits on the pedion face of a tourmaline crystal after a few minutes of etching in molten potassium hydroxide, less alkaline aqueous phases would probably also be capable of causing the observed etching phenomena with a longer exposure time and increased temperature.

– High pH values of the fluid are to be expected in alkali-rich melts.
– A temporary increase in the temperature of the miarole would also lead to an undersaturation and, consequently, corrosion. Such a temporary increase in the temperature of the entire rock mass surrounding the miarole could be caused, for example, by another melt intrusion nearby. It is not uncommon to see pegmatite veins intersecting each other in pegmatite fields, indicating that the veins formed one after the other. Finally, fluids from outside could have entered the miarole during the ascent of the pegmatite to the earth's surface, that could either lead to more tourmaline growth, or to the etching phenomena.

The second part of this contribution (Rustemeyer 2026) is a study of the inner morphology of strongly etched and then recrystallized tourmaline crystals from Skardu, Pakistan. In those crystals the bespoken etching phenomena could be discovered as complex color zones, quasi as crystalline fossils.

Acknowledgements. I am thankful to the scientific team of the TUR5 congress, Peter Bačík, Ferdinando Bosi, Barbara L. Dutrow, Darrell J. Henry, Vincent J. van Hinsberg, Milan Novak, Federico Pezzotta, and Robert B. Trumbull for the invitation as guest speaker. Thanks are addressed to Horst Marschall and Alexander Falster for giving first feedback on my manuscript. I am indebted to Horst Marschall for the thorough reviews of this manuscript leading to considerable improvements. Last but not least, I thank the guest editors Jan Cempírek and Ferdinando Bosi for their support.

References

Agheem H, Shah MT, Khan T (2004) Gems and gem-bearing pegmatites of the Shigar valley, Skardu, Northern Pakistan. Geol Bull Univ Peshawar 37: 167–178

Agheem MH, Shah MT, Khan T, Laghari A, Dars H (2011) Field features and petrography used as indicators for the classification of Shigar Valley pegmatites, Gilgit-Baltistan region of Pakistan. Himal J Earth, Sci Univ Peshawar 44: 1–7

Correns CW (1967) Einführung in die Mineralogie. Springer, pp 1–458

Dietrich RV (1985) The Tourmaline Group. Van Nostrand Reinhold, New York, N.Y., USA, pp 1–287

Dutrow BL, Henry DJ (2011) Tourmaline: A Geologic DVD. Elements 7: 301–306

Grasemann BE, Dragantis E (2003) Schatzkammer Himalaya. Extra Lapis 24: 22–26

Goldschmidt V (1922) Atlas der Kristallformen. Carl Winters Universitäts Buchhandlung, Heidelberg

Hammer V (2003) Pegmatites: Always Good for a Surprise. Extra Lapis 24: 50–63

Heimann RB (1975) Dissolution of Crystals. Springer Verlag Vienna, New York, pp 1–270

Henry DJ, Dutrow BL, Selverstone J (2003) Compositional asymmetry in replacement tourmaline—An example from the Tauern Window, Eastern Alps. Am Mineral 88: 1399–1399

Honess AP (1929) The nature, origin and interpretation of etch figures on crystals. Wiley, New York, pp 1–171

Jagoutz O, Bouilhol P, Schaltegger U, Müntener O (2018) The isotopic evolution of the Kohistan Ladakh arc from subduction initiation to continent arc collision. Geol Soc London, Spec Publ 483: SP483.7

Kazmi A, Peters JJ, Obboda HP (1985) Gilgit, Pakistan. Mineral Rec 16: 393–411

Kleber W (1967) Einführung in die Kristallographie. VEB Verlag Technik, pp 1–407

Kulaszewski C (1920) Etching and dissolution phenomena in tourmaline. Reports of the Academy of Sciences (Leipzig) 72: 48–55

Lasaga CA, Luttge A. (2001) Variation of Crystal Dissolution Rate Based on a Dissolution Stepwave model. Science 291: 2400–2404

Lasaga AC, Luttge A (2003) A model for crystal dissolution. Eur J Mineral 15: 603–615

Laurs B M, Dilles JH, Wairrach Y, KausarAB, Snee LW (1998) Geological setting and petrogenesis of symmetrically zoned, miarolitic granitic pegmatites at Stak Nala, Nanga Parbat Haramosh Massif, Northern Pakistan. Canad Mineral 36: 1–47

Li L, Wang L, Romer RL, Ma C, Cao L, Tian Y (2025) Using tourmaline to trace Li mineralization in the Mufushan granitic batholith, South China. Chem Geol 671: 122485

London D (1986) Formation of tourmaline-rich gem pockets in miarolitic pegmatites. Am Mineral 71: 396–405

London D (2008) Pegmatites. Canad Mineral, Spec Publ 10, pp 1–347

London D (2013) Crystal-Filled Cavities in Granitic Pegmatites: Bursting the Bubble. Rocks Miner 88: 527–538

London D (2016) Reading Pegmatites – part 2: What Tourmaline says. Rocks Miner 91: 132–147

Roda-Robles E, Vieira R, Lima A, Errandonea MJ, Pesquera A, Cardoso-Fernandes J, Garate-Olave I (2023) Li-rich pegmatites and related peraluminous granites of the Fregeneda–Almendra field (Spain–Portugal): A case study of magmatic signature for Li enrichment. Lithos 452–453: 107195

Rossman GR, Fritsch E, Shigley JE (1991) Origin of color in cuprian elbaite from Sao Jose de Batalha, Paraiba, Brazil. Am Mineral 76: 1479–1484

Rustemeyer P (2003) Faszination Turmalin. Spektrum Akad. Verl. Weinheim, Germany, pp 1–308

Rustemeyer P (2015) Tourmaline – Fascinating Crystals with Fantastic Inner Worlds. Verlag Dr. Friedrich Pfeil, Munich, Germany, pp 1–272

Rustemeyer P (2022) The Inner Architecture of Tourmaline Crystals as inferred from the morphology of color zones in thin slices. J Geosci 67: 103–128

Rustemeyer, P (2023) Fascinating Structures within Slices from Dark Tourmaline Crystals. Rocks Miner 98: 418–434

Rustemeyer, P (2026) Tourmaline Crystals with Corrosion Phenomena from the Skardu Area, North Pakistan. Part 2: Inner Morphology of Tourmaline crystals with corrosion and subsequent healing. J Geosci 71: 79–99

Sangwal K (1987) Etching of Crystals. Elsevier, pp 1–497

Simmons W, Webber KL, Falster AU, Roda-Robles E, Dallaire DA (2022) Pegmatology, Pegmatite Mineralogy, Petrology & Petrogenesis. 2nd edition. Rubellite Press, Cana, Virginia, pp 1–287

Slack JF, Trumbull RB (2011) Tourmaline as a recorder of ore-forming processes. Elements 7: 321–326

Thomas R. Davidson P (2012) Water in granite and pegmatite-forming melts. Ore Geology Reviews, 46: 32–46

Thomas R, Davidson P H, Beurlen H. (2012) The competing models for the origin and internal evolution of granitic pegmatites in the light of melt and fluid inclusion research. Mineral Petrol 106: 55–73

Van Hinsberg VJ, Henry DJ, Dutrow BL (2011) Tourmaline as Petrologic Forensic Mineral: A unique Recorder of Its Past. Elements 7: 327–332

Van Hinsberg VJ, Schumacher, Kearns JC, Mason S,Franz G. (2006) Hourglass sector zoning in metamorphic tourmaline and resultant major and trace-element fractionation. Am Mineral 91: 717–28

Webber K, Simmons WB, Falster AU, Foord EE (1999) Cooling rates and crystallization dynamics of shallow level pegmatite–aplite dikes, San Diego County, California. Am Mineral 84: 708–717